

Current-voltage characteristics through a single light-sensitive molecule

Chun Zhang,* Yao He, and Hai-Ping Cheng[†]

Department of Physics and Quantum Theory Project, University of Florida, Gainesville, Florida 32611

Yongqiang Xue

College of Nanoscale Science and Engineering, University at Albany—SUNY, Albany, New York 12203

Mark A. Ratner

Department of Chemistry, Northwestern University, Evanston, Illinois 60208

X.-G. Zhang and Predrag Krstic

Computer Science and Mathematics Division, Oak Ridge National Laboratory, Oak Ridge, Tennessee 37831

(Received 31 July 2005; revised manuscript received 3 October 2005; published 31 March 2006)

A light-sensitive molecular switch based on single azobenzene molecule has been proposed recently [C. Zhang, M. H. Du, H. P. Cheng, X. G. Zhang, A. E. Roitberg, and J. L. Krause, *Physical Review Letters* **92**, 158301 (2004)]. Here we investigate the stability of the molecular switch under finite bias. Using a first-principles method that combines the nonequilibrium Green's function technique and density functional theory, we compute the current-voltage curves for both *trans* and *cis* configurations of the azobenzene molecule connected to two gold leads between bias voltages of 0 and 1 V. We find that the current through the *trans* configuration is significantly higher than that through the *cis* configuration for most biases, suggesting that the molecular switch proposed previously is stable under the finite bias. A negative differential conductance (NDR) is found for the *cis* configuration at 0.8 V. Analysis of the band structure of the leads and the molecular states reveals that the transmission through the highest occupied molecular orbital state of the molecule is suppressed significantly at this bias voltage, which causes the NDR.

DOI: [10.1103/PhysRevB.73.125445](https://doi.org/10.1103/PhysRevB.73.125445)

PACS number(s): 85.65.+h, 73.63.-b, 82.37.Gk

I. INTRODUCTION

Electronic devices based on single molecules have been considered as one of the most promising technologies to extend today's semiconductor-based electronics.^{1–10} Many potentially useful molecular electronic devices have been proposed.^{2,3,11–15} Most prominent among these is a single-molecule switch^{13–15} since a switch is a critical element of any modern design of logical and memory circuits. In a previous work,¹⁴ we proposed a light-driven molecular switch consisting of a single azobenzene molecule connected to two semi-infinite Au leads via two linker S atoms. The azobenzene molecule has two stable configurations: the *trans* and the *cis* states. In the linear response regime, the *trans* configuration was shown to have a significantly higher conductance than the *cis* configuration. Since the molecule can be switched reversibly from one configuration to the other by photoexcitation,^{16–18} it is a promising candidate for the light-driven molecular switch. In this paper we will examine the stability of this switching behavior under a finite bias voltage.

Applying a finite bias voltage V_b , the Fermi energies deep in both leads are shifted by $\pm V_b/2$, respectively, which changes the electrostatic potential and correspondingly the effective single-particle potential in the device area. We include a sufficiently large proportion of the leads into the active device region. The electronic potential deep in the two leads far away from the device region is, then, not affected by the electron interactions in the device area. The nonlinear transport characteristics are computed using first-principles

methods,^{15,19–21} which combine the nonequilibrium Green's functions technique of quantum transport^{22,23} with the density functional theory (DFT) of the device electronic structure.²⁴

II. THEORETICAL APPROACH

Transport studies deal with open systems that are connected to two (or more) external reservoirs. Within the regime of coherent transport, this is studied using the scattering theory introduced by Landauer and Buttiker.^{25,26} In this approach, the transport system under study is divided into three parts—left lead, right lead, and the scattering region or the device area—which also includes portions of two electrodes to take into account of the molecule-lead coupling and the lead screening effect. Applying a finite bias voltage shifts the Fermi energies of the two leads relative to each other $V_b = \mu_R - \mu_L$ (without losing generality, we assume that $\mu_R > \mu_L$), where μ_R and μ_L are the Fermi energies of right and left leads, respectively. The bias voltage enters the calculation via shifts in the electrostatic potential in the left lead by the amount of $-V_b/2$ and the right lead by $V_b/2$, which forms the boundary condition for studying the charge and potential response of the device region.²⁰ The electronic structure of the leads is obtained through two separate lead calculations, from which we obtain two self-energy terms, Σ_L and Σ_R , due to the left and right leads, respectively, using standard procedures.^{27,28} A self-consistent procedure based on DFT is used to calculate the effective single-particle po-

tential in the device area. We outline briefly the procedure of calculations below.^{19,20}

The most important physical quantity in the framework of DFT is the electron density. Given the electron density ρ in the device area, the effective potential V_{eff} and the Hamiltonian \hat{H}_{Cen} of the device area can be computed as a functional of the density. Once we know the effective potential, the nonequilibrium Green's function $G^<$ can be calculated as

$$G^< = f_+ G^r \Gamma^L G^a + f_- G^r \Gamma^R G^a, \quad (1)$$

where f_+ and f_- are Fermi-Dirac distribution functions for right and left leads, respectively. The retarded and advanced Green's functions are calculated as

$$G^{r(a)} = \frac{1}{E - \hat{H}_{Cen} - (\Sigma_L^{r(a)} + \Sigma_R^{r(a)})}. \quad (2)$$

The spectral width functions Γ^L and Γ^R are defined as

$$\Gamma^{L(R)} \equiv i \left(\Sigma_{L(R)}^r - \Sigma_{L(R)}^a \right). \quad (3)$$

The electron density is related to $G^<$ by a simple relation

$$\rho = \frac{1}{2\pi i} \int G^<(\varepsilon) d\varepsilon. \quad (4)$$

The procedure is repeated until the self-consistency is achieved.

After reaching self-consistency, the transmission probability as a function of the bias voltage and the energy can be computed using the Caroli formula^{19,20,29}

$$T(\varepsilon, V_b) = \text{Tr}[\Gamma^L(\varepsilon, V_b) G^r(\varepsilon, V_b) \Gamma^R(\varepsilon, V_b) G^a(\varepsilon, V_b)]. \quad (5)$$

At zero temperature, the current can be expressed as an integral of the transmission probability,

$$J = \frac{2e}{h} \int_{\mu_L}^{\mu_R} d\varepsilon T(\varepsilon, V_b). \quad (6)$$

III. APPLICATION TO Au/S/AZOBENZENE/S/Au SYSTEM

The azobenzene molecular switch consists of two Au nanowires connected by a single azobenzene molecule as shown in Fig. 1(a). The contacts between the molecule and two nanowires are provided by CH_2S groups. We neglect possible bias voltage-induced structural change of the molecule and take the same configuration as in the previous work,¹⁴ where we use a fully quantum calculation to optimize the structure of the device area; the interlead distances were found to be 18.16 Å for the *trans* and 16.23 Å for the *cis* configuration, respectively. The band structure of the wire is shown in Fig. 1(b). The 5.3 eV Fermi energy (5.7 eV for bulk system) is due to the artificial construction of the gold wire and the model we use to calculate the band structure. However, all calculations are performed consistently within the model. Note that only one band is crossing the Fermi level.

In this work, for nonequilibrium approach, we use the BPW91 parameterization of the exchange-correlation

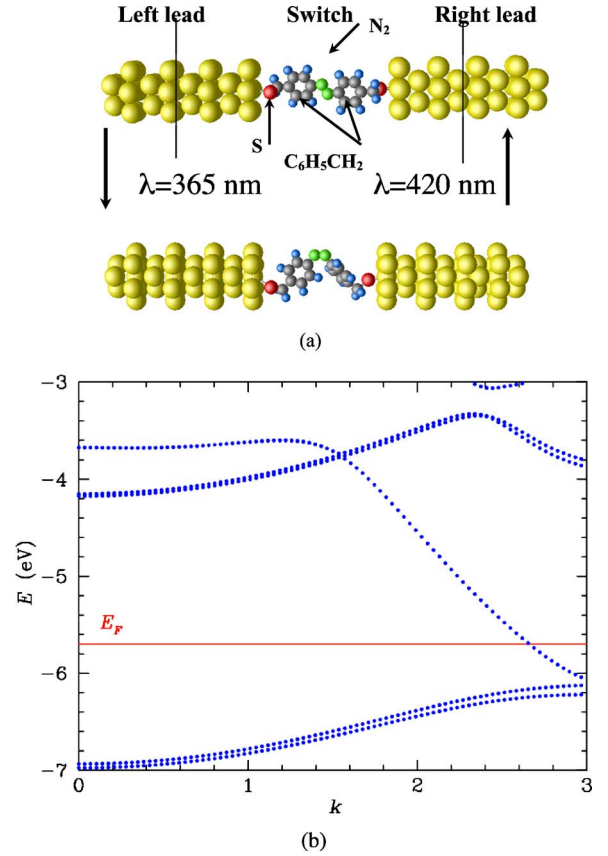


FIG. 1. (Color online) Panel (a) is the device structure of the molecular switch that consists of two gold leads and an azobenzene molecule. Top: the *trans* configuration. Bottom: the *cis* configuration. (b) Band structure of the model quasi-one-dimensional gold wire. Note that only one band goes across the Fermi energy.

functional.³⁰ The chosen pseudopotential is CEP-31G with corresponding Gaussian basis set for the azobenzene molecule³¹ and LANL1MB for gold leads.³²

The nonequilibrium first-principles approach allows the self-consistent calculation of the electrostatic potential as a function of the external bias. As an example, we show in Fig. 2 the difference in the electrostatic potentials between 0 and 1 V for the *cis* configuration. The y axis is along the current direction and the x - z plane is parallel to the N double bond, cutting through the midpoint of the Au unit cell. The drop in the electrostatic potential across the switch area can be seen clearly in the figure.

The current through the system is calculated with Eq. (6), as an integral of the electron transmission probability over energy. The effects of external bias voltage on the current through the switch enter in two ways. First, the upper and lower limits of the integral change with increasing bias voltage so that more possible channels enter the integral. Second, the bias voltage may change the transmission probability at each energy: As the external bias changes, the effective Kohn-Sham potential in the device region changes due to the change of electron density distribution, which modifies both the wave-function character and the energy level of the “molecular orbital;”³³ in addition, the external bias shifts the Fermi energies of the two leads in opposite directions so that

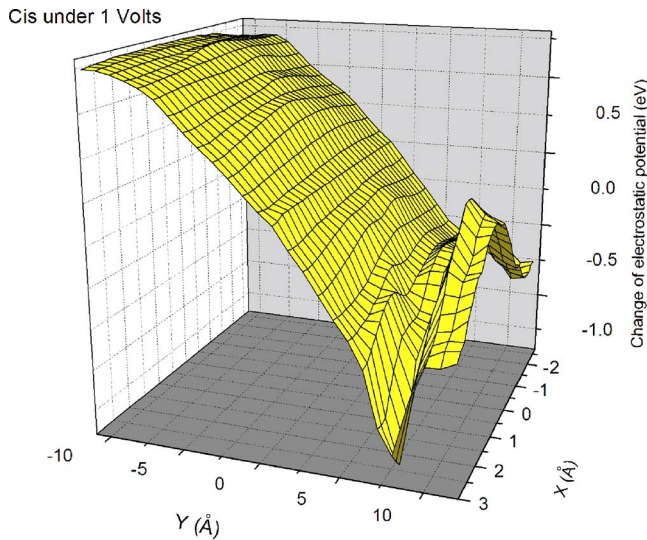


FIG. 2. (Color online) The difference in electrostatic potential between 0 and 1 V biases for the *cis* configuration. The x - z plane is parallel to the N_2 bond, cutting through the midpoint of the Au unit cell.

the individual molecular orbitals couple to different energy channels in both leads as a function of the applied bias. All of these effects are taken into account in the first-principles treatment. In Fig. 3, we show the transmission probability, calculated from Eq. (5), as a function of both energy and bias voltage for the *cis* configuration.

I - V curves through both the *trans* and *cis* configurations are shown in Fig. 4. For bias voltages below one volt, the current through the *trans* configuration is significantly higher than the current through the *cis* configuration. This difference is about two orders of magnitude for bias voltages below 0.3 V, suggesting that the switching behavior is stable under a small bias voltage. Another interesting feature in Fig. 4 is

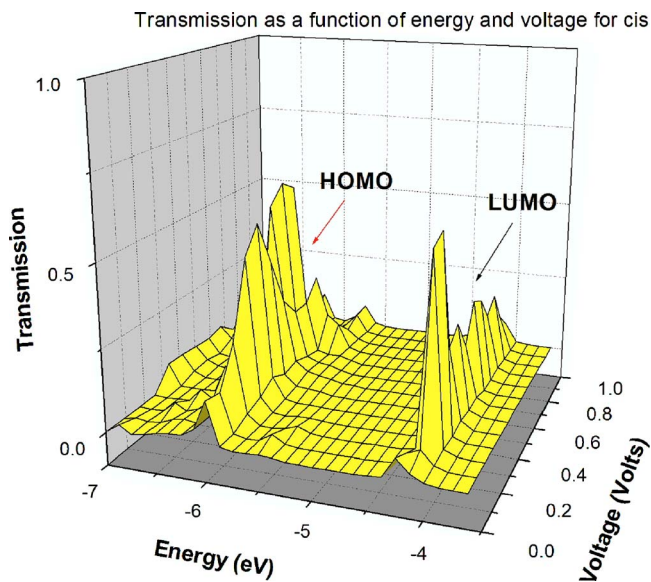


FIG. 3. (Color online) Transmission probability as a function of energy and the external bias voltage for the *cis* configuration.

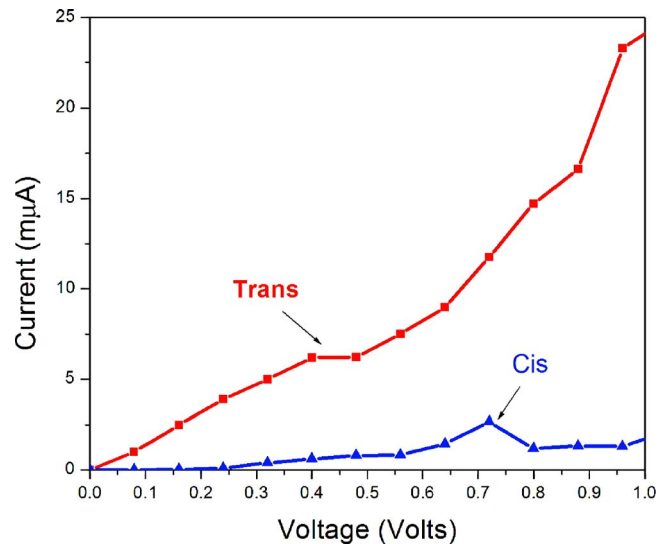


FIG. 4. (Color online) Current as a function of bias voltage for both *trans* and *cis* configurations. The top line represents the current for *trans* and the bottom line is for *cis*.

that between 0.72 and 0.8 V, the current through the *cis* molecule decreases significantly with increasing voltage. The differential conductance, defined as the derivative of the current with respect to the bias voltage, is shown in Fig. 5 and is clearly negative at 0.8 V for the *cis* molecule. The zero-bias differential conductance of the *trans* configuration is two orders of magnitude higher than that of the *cis*, in agreement with the linear response study.¹⁴

The weak negative differential conductance has been understood as due to the off alignment of the resonant state and the Fermi level of electrodes in the semiconductor heterostructure,³⁴ and as the off-alignment of density of states of the scanning tunneling microscope (STM) tip and the substrate in an STM experiment.³⁵ For elastic transport through one-dimensional molecular junctions, NDR is more frequently observed and can have different mechanisms,^{36–38} including a vibronic one.^{37,38} Normally, as the bias voltage

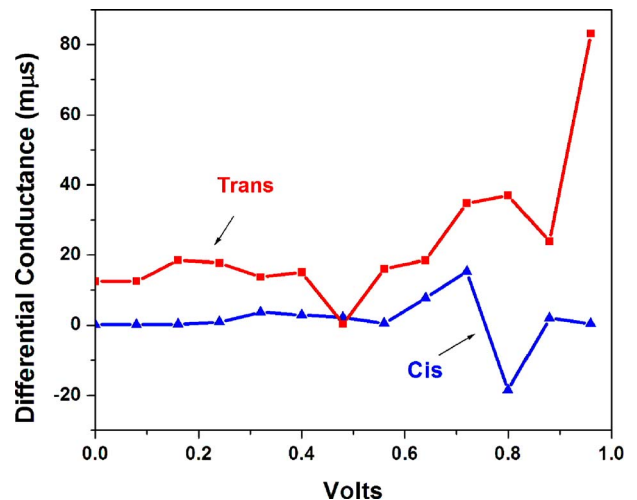


FIG. 5. (Color online) The differential conductance as a function of bias voltage for both *trans* and *cis* configurations.

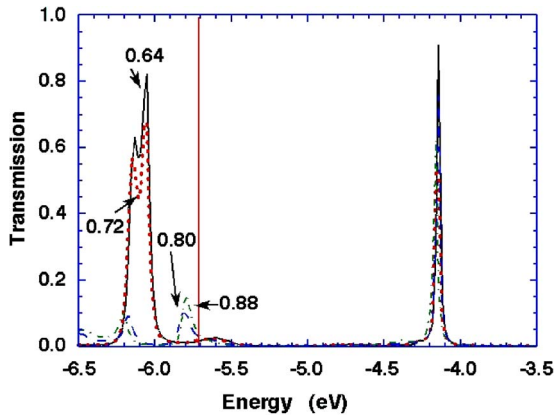


FIG. 6. (Color online) Transmission coefficient as a function of energy of the *cis* configuration at external bias voltages of 0.64, 0.72, 0.8, and 0.88 V, in solid, dotted, dashed, and dotted-dashed lines, respectively. The solid vertical line indicates the Fermi energy.

increases, more transport channels enter the integral of Eq. (6), which increases the current. However, the electron transmission probability is determined by the wave-function character of the electron channels in the leads, the wave-function character of the molecular orbital and their coupling strength. If a mismatch between a conduction channel in the leads and a molecular orbital occurs due to the energy shifts induced by the bias voltage, electron transmission in the corresponding energy range can be significantly suppressed. Such a decrease in the electron transmission may not be compensated by the increase in the number of channels. Figure 6 clearly indicates such an example. We plot the transmission as a function of energy for bias voltages 0.64, 0.72, 0.8, and 0.88 V. The Fermi energy of leads at zero bias is -5.72 eV. Then, the integration windows (μ_L, μ_R) in Eq. (6) for those bias voltages are $(-6.04, -5.40)$, $(-6.08, -5.36)$, $(-6.12, -5.32)$, $(-6.16, -5.28)$ eV, respectively. From 0.64 to 0.72 V, the transmission through the highest occupied molecular orbital (HOMO) state decreases a little bit. However, the HOMO state is not included in the energy window at 0.64 V, and transmissions at other energies within the window at 0.64 V see little change; thus, the wider energy window at 0.72 V gives a higher current than that at 0.64 V.

At 0.8 V, the external bias changes the HOMO state significantly. The energy of the HOMO state shifts from -6.1 to -5.8 eV, and the transmission through this state is drastically suppressed, which decreases the total current and yields a NDR.

Another important feature we can see from the Fig. 6 is that the bias voltage has little effect on the position of the lowest unoccupied molecular orbital (LUMO) state, while the HOMO state shifts at certain bias voltages. The reason is that the LUMO state is more localized in the molecule. A simple quantum chemical calculation shows that the LUMO state of the azobenzene molecule is mainly localized around N=N double bond. Our previous study¹⁴ showed that around the energy of HOMO state, there are significant density of states at both two benzene rings and two unit cells of leads connected to the molecule while the density of states at N=N double bond is low. Thus, the shift of the Fermi energy of leads has significant effects on the HOMO state.

IV. SUMMARY

We present a study of the transport properties of Au/S/Azobenzene/S/Au system under finite bias using a first-principles method that combines the nonequilibrium Green's function techniques and static-DFT treatment of the device electronic structure. Our calculation shows that for bias voltages below one volt, the current through the *trans* configuration is significantly higher than that of the *cis* configuration, and suggests that the light-sensitive switching behavior is stable under small bias voltages. We also found that at 0.8 V, a negative differential conductance results from a shift in the energy of the HOMO state of the molecule.

ACKNOWLEDGMENT

This work is supported by DOE BES under Contract No. FG02-02ER45995 and is a user project at the CNMS operated by Division of User Facilities, US DOE at ORNL. Y. X. is partially supported by the DoD-DURINT program through ARO and MARCO/DARPA Interconnect Focus Center. M. R. is grateful to the NSF/NCN program for support through Purdue University. We also acknowledge DOE/NERSC and CNMS at ORNL for computer time.

*Present address: School of Physics, Georgia Institute of Technology, Atlanta, GA 30332

†Corresponding author. Email address: cheng@qtp.ufl.edu

¹A. Aviram and M. A. Ratner, *Chem. Phys. Lett.* **29**, 277 (1974).

²M. A. Reed and L. Takhee (American Scientific Publishers, Stevenson Ranch, CA, 2003).

³J. R. Heath and M. A. Ratner, *Phys. Today* **56**(5), 43 (2003).

⁴C. Joachim, J. K. Gimzewski, R. R. Schlittler, and C. Chavy, *Phys. Rev. Lett.* **74**, 2102 (1995).

⁵S. J. Tans, M. H. Devoret, H. J. Dai, A. Thess, R. E. Smalley, L. J. Geerligs, and C. Dekker, *Nature (London)* **386**, 474 (1997).

⁶F. Moresco, G. Meyer, K. H. Rieder, H. Tang, A. Gourdon, and

C. Joachim, *Phys. Rev. Lett.* **86**, 672 (2001).

⁷J. M. Seminario, P. A. Derosa, and J. L. Bastos, *J. Am. Chem. Soc.* **124**, 10266 (2002).

⁸R. Gutierrez, G. Fagas, G. Cuniberti, F. Grossmann, R. Schmidt, and K. Richter, *Phys. Rev. B* **65**, 113410 (2002).

⁹P. Orellana and F. Claro, *Phys. Rev. Lett.* **90**, 178302 (2003).

¹⁰E. G. Emberly and G. Kirczenow, *Phys. Rev. Lett.* **91**, 188301 (2003).

¹¹M. A. Reed, C. Zhou, C. J. Muller, T. P. Burgin, and J. M. Tour, *Science* **278**, 252 (1997).

¹²J. R. Heath, J. F. Stoddart, and R. S. Williams, *Science* **303**, 1136 (2004).

- ¹³J. Li, G. Speyer, and O. F. Sankey, Phys. Rev. Lett. **93**, 248302 (2004).
- ¹⁴C. Zhang, M. H. Du, H. P. Cheng, X. G. Zhang, A. E. Roitberg, and J. L. Krause, Phys. Rev. Lett. **92**, 158301 (2004).
- ¹⁵J. Taylor, H. Guo, and J. Wang, Phys. Rev. B **63**, R121104 (2001).
- ¹⁶T. Hugel, N. B. Holland, A. Cattani, L. Moroder, M. Seitz, and H. E. Gaub, Science **296**, 1103 (2002).
- ¹⁷T. Seki, J. Y. Kojima, and K. Ichimura, J. Phys. Chem. B **103**, 10338 (1999).
- ¹⁸S. Yasuda, T. Nakamura, M. Matsumoto, and H. Shigekawa, J. Am. Chem. Soc. **125**, 16430 (2003).
- ¹⁹J. Taylor, H. Guo, and J. Wang, Phys. Rev. B **63**, 245407 (2001).
- ²⁰Y. Q. Xue, S. Datta, and M. A. Ratner, Chem. Phys. **281**, 151 (2002).
- ²¹M. Brandbyge, J. Schiøtz, M. R. Sørensen, P. Stoltze, K. W. Jacobsen, J. K. Nørskov, L. Olesen, E. Laegsgaard, I. Stensgaard, and F. Besenbacher, Phys. Rev. B **52**, 8499 (1995).
- ²²S. Datta, Superlattices Microstruct. **28**, 253 (2000).
- ²³S. Datta, *Electronic Transport in Mesoscopic System* (Cambridge University Press, Cambridge, UK, 2002).
- ²⁴W. Kohn and L. J. Sham, Phys. Rev. A **140**, 1133 (1965).
- ²⁵M. Buttiker, Phys. Rev. Lett. **57**, 1761 (1986).
- ²⁶A. D. Stone and A. Szafer, IBM J. Res. Dev. **32**, 384 (1988).
- ²⁷P. S. Krstic, X. G. Zhang, and W. H. Butler, Phys. Rev. B **66**, 205319 (2002).
- ²⁸S. Sanvito, C. J. Lambert, J. H. Jefferson, and A. M. Bratkovsky, Phys. Rev. B **59**, 11936 (1999).
- ²⁹C. Caroli, R. Combescio, P. Nozieres, and D. Saintjam, J. Phys. C **4**, 916 (1971).
- ³⁰A. D. Becke, Phys. Rev. A **38**, 3098 (1988).
- ³¹W. J. Stevens, H. Basch, and M. Krauss, J. Chem. Phys. **81**, 6026 (1984).
- ³²P. J. Hay and W. R. Wadt, J. Chem. Phys. **82**, 270 (1985).
- ³³Y. Q. Xue and M. A. Ratner, Phys. Rev. B **68**, 115406 (2003).
- ³⁴H. Heinrich, G. Bauer, and F. Kucher, in *Springer Series in Solid State Sciences*, vol. 83 (Springer-Verlag, Berlin, 1988).
- ³⁵I. W. Lyo and P. Avouris, Science **245**, 1369 (1989).
- ³⁶Y. Q. Xue, S. Datta, S. Hong, R. Reifengerger, J. I. Henderson, and C. P. Kubiak, Phys. Rev. B **59**, R7852 (1999).
- ³⁷A. Troisi, M. A. Ratner, and A. Nitzan, J. Chem. Phys. **118**, 6072 (2003).
- ³⁸M. Galperin, M. A. Ratner, and A. Nitzan, J. Chem. Phys. **121**, 11965 (2004).